Functional A posteriori error estimation for stationary reaction-convection-diffusion problems

Eigel, Martin ; Samrowski, Tatiana

Abstract: A functional type a posteriori error estimator for the finite element discretization of the stationary reaction-convection-diffusion equation is derived. In case of dominant convection, the solution for this class of problems typically exhibits boundary layers and shock-front like areas with steep gradients. This renders the accurate numerical solution very demanding and appropriate techniques for the adaptive resolution of regions with large approximation errors are crucial. Functional error estimators as derived here contain no mesh-dependent constants and provide guaranteed error bounds for any conforming approximation. To evaluate the error estimator, a minimization problem is solved which does not require any Galerkin orthogonality or any specific properties of the employed approximation space. Based on a set of numerical examples, we assess the performance of the new estimator. It is observed that it exhibits a good efficiency also with convection-dominated problem settings.

DOI: https://doi.org/10.1515/cmam-2014-0005

Computational Methods in Applied Mathematics
Vol. 14 (2014), No. 2, pp. 135–150

Doi: 10.1515/cmam-2014-0005

DE GRUYTER

Functional A Posteriori Error Estimation for Stationary Reaction-Convection-Diffusion Problems

Martin Eigel · Tatiana Samrowski

Abstract — A functional type a posteriori error estimator for the finite element discretization of the stationary reaction-convection-diffusion equation is derived. In case of dominant convection, the solution for this class of problems typically exhibits boundary layers and shock-front like areas with steep gradients. This renders the accurate numerical solution very demanding and appropriate techniques for the adaptive resolution of regions with large approximation errors are crucial. Functional error estimators as derived here contain no mesh-dependent constants and provide guaranteed error bounds for any conforming approximation. To evaluate the error estimator, a minimization problem is solved which does not require any Galerkin orthogonality or any specific properties of the employed approximation space. Based on a set of numerical examples, we assess the performance of the new estimator. It is observed that it exhibits a good efficiency also with convection-dominated problem settings.

2010 Mathematical subject classification: 65N30, 65N15, 65J15, 65N22, 65J10.

Keywords: A Posteriori Error Analysis, Finite Element Method, Adaptivity, Dominant Convection, Functional Estimator.

1. Introduction

The aim of this paper is to derive a functional type a posteriori error estimator for the reaction-convection-diffusion equation of the form

$$-\operatorname{div} A\nabla u + a\cdot\nabla u + \rho^2 u = f$$

defined on some Lipschitz domain $\Omega\subset\mathbb{R}^2$. This equation describes the transport of some scalar quantity u by a diffusion with coefficient A, a convection with regard to vector field a and some reaction with coefficient ρ^2 which models creation or depletion of the quantity u. The term f on the right-hand side models a source or sink. We assume the coefficients to be chosen appropriately for a solution to exist. In practical applications, the convection often dominates the process and makes the problem difficult to solve accurately numerically. This is due to so-called layers which arise in the solution. These are regions where the solution exhibits steep gradients which present a serious challenge for numerical (and also analytical)

Martin Eigel
Weierstrass Institute, Mohrenstr. 39, 10117 Berlin, Germany
E-mail: martin.eigel@wias-berlin.de.

Tatiana Samrowski
Zurich University of Applied Sciences, Technikumstrasse 9, 8400 Winterthur, Switzerland
E-mail: samo@zhaw.ch.

methods. Layers can appear within the domain as well as at the boundaries. Since they are critical for an accurate approximation of the solution, adequate techniques to resolve such layers are required. A possible approach is the application of a posteriori error estimators. These can be used to steer an adaptive mesh refinement with the aim to identify regions where the error of the approximation is high. Moreover, they provide a measure for the quality of the numerical approximation.

Adaptivity in the numerical solution for partial differential equation has become a common requirement in practical computations and a broad range of estimators has been developed, see, e.g., [2,3,13,26]. In recent years, the goal to derive sharp bounds without unknown constants has evolved and lead to some very efficient estimators which are often based on flux equilibration techniques. Functional type error estimators as presented in this work were introduced in [16–18] and further developed in a series of articles and books, see [20, 22, 25] and also [23, 24]. In these error estimators, Galerkin orthogonality of the numerical solution is not required and they can be derived without unknown constants in the estimate. For the model equation used in this article, recent advances in this area [21] have not yet been applied and demonstrated which we intend to remedy. It is shown that reliable, efficient and robust functional error estimators can be derived for the reaction-convection-diffusion problem.

For an adaptive refinement algorithm, an error estimator η can be used, if η identifies the regions in the domain where the numerical solution u_h should be improved, i.e., where the approximation error $e := u - u_h$ is large. This requires the error estimator to be defined by local contributions η_T on all elements $T \in \mathcal{T}$ such that

$$\eta^2 := \sum_{T\in\mathcal{T}} \eta_T^2.$$

The aim is to control the global error e in some norm $|||\cdot|||$ such that

$$|||e||| < \varepsilon$$

with some small $\varepsilon > 0$. An adaptive algorithm based on the error estimator η stops when the threshold ε is reached, i.e., the solution has achieved sufficient accuracy.

For the examined second order equations, the discrete solution may deteriorate at local singularities which, e.g., arise from boundary layers, sharp shock-like fronts or corners in the domain. The mesh is expected to be adaptively refined in such critical areas of the domain. This will be examined in the numerical examples in Section 4. It turns out that the adapted meshes produced on the basis of the functional error estimator resolve the layers of the problems very precisely.

Notation

Throughout this paper, we use the common notation for Sobolev spaces defined on a domain Ω (see [1,4,5]). The space of quadratic summable functions is denoted by $L^2(\Omega)$, the Sobolev space $H^1(\Omega)$ of functions with additional L^2 summable first order weak derivatives. The L^2 scalar product is denoted by $(u, v) := \int_\Omega uv\,dx$ and the induced norm by $\|\cdot\|$. Moreover, let

$$H_0^1(\Omega) := \left\{v \in H^1(\Omega) \mid v|_{\partial\Omega} = 0\right\}$$

and

$$H(\Omega, \mathrm{div}) := \left\{y \in L^2(\Omega, \mathbb{R}^2) \mid \mathrm{div}\, y \in L^2(\Omega)\right\}.$$

We assume a piecewise domain $\Omega \subset \mathbb{R}^2$ and its regular partition $\mathcal{T}$ into triangles $T \in \mathcal{T}$ with edges $E \in \mathcal{E}$ and the set of vertices $\mathcal{N}$. Any two triangles of $\mathcal{T}$ share at most one common edge or two vertices and all triangles are shape regular, i.e., the ratio of the smallest circumscribed circle and the largest circle inscribed is bounded by a constant which does not depend on the triangle for any $T \in \mathcal{T}$. We denote by h the mesh-size function which is defined by $h := h_T := \operatorname{diam}(T)$ on $T \in \mathcal{T}$. The jump of $v \in L^2(\Omega)$ along some edge $E \in \mathcal{E}$ is denoted by $[v]_E$ and the outer unit normal vector with regard to E is denoted by ν_E.

The patch of some node $z \in \mathcal{N}$ or an edge $E \in \mathcal{E}$ is defined by $\omega_z := \{T \in \mathcal{T} \mid z \in T\}$ or $\omega_E := \{T \in \mathcal{T} \mid E \in T\}$, respectively. Moreover, we define the discrete spaces

$$V_h := \left\{v \in C(\overline{\Omega}) \mid v|_T \in P_1(T) \text{ for all } T \in \mathcal{T}, \text{ and } v = 0 \text{ on } \Gamma_D\right\} \quad \text{and} \quad V_h^2 := V_h \times V_h,$$

where P_k, $k \in \mathbb{N}$, is the space of polynomials of maximal degree k.

Outline

The paper is organized as follows. In the next section, we define the reaction-convection-diffusion equation and required properties. Moreover, we introduce a classic stabilized FEM discretization for convection dominated problems, the streamline diffusion method (SDM, see [11]). In Section 3, our new functional type a posteriori error estimator is derived. The numerical experiments of Section 4 demonstrate the performance of our estimator with a set of benchmark problems.

2. Model Problem and Discretization

In this section, we introduce the model problem under consideration and describe a stabilized discretization with the finite element method (FEM).

2.1. Model Problem

We consider the stationary linear reaction-convection-diffusion problem

$$\begin{aligned} -\operatorname{div} A\nabla u + a \cdot \nabla u + \rho^2 u &= f \quad \text{in } \Omega, \\ u &= u_0 \quad \text{on } \Gamma_D, \\ A\nabla u \cdot n &= F \quad \text{on } \Gamma_N \end{aligned} \tag{2.1}$$

on a connected bounded domain $\Omega \subset \mathbb{R}^2$ with Lipschitz boundary $\Gamma = \Gamma_D \cup \Gamma_N$, $\Gamma_D \cap \Gamma_N = \emptyset$, consisting of some Neumann boundary part Γ_N and some Dirichlet boundary Γ_D of positive measure $\operatorname{meas}(\Gamma_D) > 0$. The Dirichlet boundary function u_0 is assumed to be sufficiently smooth and well approximated on Γ_D in the discrete space of the solution. Moreover, we assume f and F to be sufficiently smooth. The diffusion tensor $A = (a_{ij})$, $i, j = 1, 2$, is symmetric and positive definite with

$$c_1|\xi|^2 \leqslant A\xi \cdot \xi \leqslant c_2|\xi|^2 \quad \text{for any } \xi \in \mathbb{R}^2. \tag{2.2}$$

The vector-valued function a satisfies the conditions

$$a \in L^\infty(\Omega, \mathbb{R}^2), \quad \operatorname{div} a \in L^\infty(\Omega), \quad \operatorname{div} a \leqslant 0$$

and

$$\rho \in L^\infty(\Omega), \quad \rho < \rho_\oplus, \quad -\frac{1}{2}\mathrm{div} a + \rho^2 =: \lambda^2 \geqslant \lambda_0^2.$$

We set

$$\kappa(x) := \frac{1}{2}(a \cdot n)(x),$$

and assume that the function κ is defined at almost all points on the boundary Γ. Moreover, the inflow part of the boundary is a subset of Γ_D, i.e., $\{x \in \Gamma \mid (a \cdot n)(x) < 0\} \subset \Gamma_D$.

The solution u of (2.1) is defined as a function in the space $V_0 + u_0$, where

$$V := H^1(\Omega) \quad \text{and} \quad V_0 := \{v \in V \mid v = 0 \text{ on } \Gamma_D\}.$$

The variational formulation of (2.1) reads: Find $u \in V_0 + u_0$ such that

$$a(u, w) = \ell(w) \quad \text{for all } w \in V_0 \tag{2.3}$$

with

$$a(u, w) := (A\nabla u, \nabla w) + (a \cdot \nabla u + \rho^2 u, w), \quad \ell(w) := (f, w) + (F, w)_{\Gamma_N}.$$

One can prove by standard arguments that the solution $u \in V_0 + u_0$ of (2.3) exists and is unique, cf. [4, 5]. Furthermore, u continuously depends on the data with respect to the energy norm defined by

$$|[u - v]| := \Big(|||\nabla(u - v)|||^2 + \int_\Omega \lambda^2 (u - v)^2 dx + \int_{\Gamma_N} \kappa (u - v)^2 ds \Big)^{1/2}. \tag{2.4}$$

Here,

$$|||q||| := \Big(\int_\Omega Aq \cdot q \, dx \Big)^{1/2} \tag{2.5}$$

for any vector-valued function $q \in L^2(\Omega, \mathbb{R}^2)$. We also introduce the norm

$$|||q|||_* := \Big(\int_\Omega A^{-1} q \cdot q \, dx \Big)^{1/2}$$

which is equivalent to the norm (2.5) due to (2.2).

2.2. FEM Discretization

With some discrete approximation $u_{h,0} \in V_h$ of the Dirichlet data u_0, we consider the FEM discretization of the weak formulation (2.3): Find $u_h \in V_h + u_{h,0}$ such that

$$a(u_h, v_h) = \ell(v_h) \quad \text{for all } v_h \in V_h. \tag{2.6}$$

For the common case of dominant convection, the standard finite element method (FEM) is not a stable discretization. This can be observed by the appearance of spurious oscillations in the solution. To circumvent this unphysical behavior, the stability of the discretization is increased by the addition of artificial diffusion to the standard weak form of the (hyperbolic) problem. For this, as a common and established stabilization technique, we recall the streamline diffusion method (SDM). We refer to [6, 11, 12] for details on the SDM and also to [8, 9] for the streamline-upwind Petrov–Galerkin method (SUPG).

The numerical experiments in Section 4 employ the standard SDM which exhibits good stability properties and high order accuracy. Instead of a test function v as noted above, we now use w which has an additional modification term that accounts for the vector field a,

$$w = v + \delta a \cdot \nabla v.$$

Several choices for the scaling δ are discussed in the literature. Usually it is expressed as a function of the local Péclet number Pe^h which depends on the local mesh size h_T and the coefficient a,

$$\delta = \frac{h_T}{2|a|}\zeta(\mathrm{Pe}^h).$$

For our computations we use $\zeta(\mathrm{Pe}^h) := \max\{0, 1 - 1/(2\mathrm{Pe}^h)\}$ as in [15], also see [6].

With the SDM discretization, the modified bilinear and linear forms for the system (2.6) read

$$\begin{aligned} a_{\mathrm{SDM}}(u_h, v_h) &:= a(u_h, v_h) - \sum_{T\in\mathcal{T}} (\operatorname{div} A\nabla u_h, \delta a \cdot \nabla v_h)_T + (a \cdot \nabla u_h + \rho^2 u_h, \delta a \nabla v_h), \\ \ell_{\mathrm{SDM}}(v_h) &:= \ell(v_h) + (f, \delta a \cdot \nabla v_h). \end{aligned}$$

3. Functional Error Estimator

3.1. General Upper Bound of the Energy Norm

In this section, we are concerned with a general functional a posteriori error estimator for reaction-convection-diffusion problems of the form (2.1). For the reader's convenience, we recall the derivation of this general estimate which was presented in [14, 22]. At first, we observe that for any $v \in V$

$$\begin{aligned} \int_\Omega (\operatorname{div} a)(u-v)^2\,dx &= \int_{\Gamma_N} a \cdot n (u-v)^2\,ds - \int_\Omega a \cdot \nabla (u-v)^2\,dx \\ &= \int_{\Gamma_N} 2\kappa (u-v)^2\,ds - \int_\Omega 2(a \cdot \nabla(u-v))(u-v)\,dx, \end{aligned}$$

and, therefore,

$$\int_\Omega \big((a \cdot \nabla(u-v))(u-v) + \rho^2(u-v)^2\big)\,dx = \int_\Omega \lambda^2 (u-v)^2 dx + \int_{\Gamma_N} \kappa (u-v)^2 ds. \tag{3.1}$$

As exemplified in [14, 22], with $w = u - v$, the weak formulation (2.3) of the reaction-convection-diffusion problem has the form

$$\begin{aligned} &\int_\Omega \big(A\nabla(u-v)\cdot\nabla(u-v) + (a\cdot\nabla(u-v))(u-v) + \rho^2(u-v)^2\big)\,dx \\ &\quad = \int_\Omega (f - (a\cdot\nabla v) - \rho^2 v)(u-v)\,dx - \int_\Omega A\nabla v \cdot \nabla(u-v)\,dx + \int_{\Gamma_N} F(u-v)\,ds. \end{aligned} \tag{3.2}$$

We deduce with (3.1) that the left-hand side of (3.2) is equivalent to the squared energy norm (2.4). We recall that for all

$$y \in Q := H(\Omega, \operatorname{div}) = \big\{q \in L^2(\Omega, \mathbb{R}^2) \mid \operatorname{div} q \in L^2(\Omega),\ q \cdot n \in L^2(\Gamma_N)\big\}$$

the following equation holds:

$$\int_\Omega (w \operatorname{div} y + y \cdot \nabla w)\, dx = \int_{\Gamma_N} (y \cdot n) w\, ds \quad \text{for all } w \in V_0 := H_0^1(\Omega).$$

Thus, (3.2) yields the following representation of the energy norm:

$$|[u-v]|^2 = \int_\Omega r_\Omega(v,y)(u-v)\, dx + \int_\Omega (y - A\nabla v)\cdot\nabla(u-v)\, dx + \int_{\Gamma_N} (F - y\cdot n)(u-v)\, ds \quad (3.3)$$

with

$$r_\Omega(v,y) := f - a\cdot\nabla v - \rho^2 v + \operatorname{div} y.$$

We denote the first term of (3.3) by

$$I_1 := \int_\Omega r_\Omega(v,y)(u-v)\, dx.$$

Application of Hölder and Friedrichs' inequalities yields

$$\begin{aligned} I_1 &= \mu \int_\Omega r_\Omega(v,y)(u-v) dx + (1-\mu)\int_\Omega r_\Omega(v,y)(u-v)\, dx \\ &\leqslant \mu \int_\Omega r_\Omega(v,y)(u-v) dx + (1-\mu)\|r_\Omega(v,y)\|_{L^2(\Omega)} c_1^{-1} C_{F,\Omega} |||\nabla(u-v)|||, \end{aligned} \quad (3.4)$$

where $0 \leqslant \mu \leqslant 1$ and $C_{F,\Omega}$ is the Friedrichs' constant defined by

$$C_{F,\Omega} := \sup_{w\in V_0\setminus\{0\}} \frac{\|w\|_\Omega}{\|\nabla w\|_\Omega}.$$

If we set $\mu = 0$ in case of $\lambda = 0$ and choose μ arbitrarily in $(0,1)$ in all other cases, the values of the integral (3.4) can be estimated by

$$I_1 \leqslant \mu \Big\| \frac{1}{\lambda} r_\Omega(v,y) \Big\|_{L^2(\Omega)} \|\lambda(u-v)\|_{L^2(\Omega)} + (1-\mu)\|r_\Omega(v,y)\|_{L^2(\Omega)} c_1^{-1} C_{F,\Omega} |||\nabla(u-v)|||. \quad (3.5)$$

For the second integral of (3.3), we set

$$I_2 := \int_\Omega (y - A\nabla v)\cdot\nabla(u-v)\, dx$$

and find by the Hölder inequality

$$I_2 \leqslant |||y - A\nabla v|||_* |||\nabla(u-v)|||. \quad (3.6)$$

Finally, we define

$$I_3 := \int_{\Gamma_N} (F - y\cdot n)(u-v)\, ds$$

and obtain for $0 \leqslant \nu \leqslant 1$

$$I_3 \leqslant \nu \int_{\Gamma_N} (F - y\cdot n)(u-v)\, ds + (1-\nu)\|(F-y\cdot n)\|_{L^2(\Gamma_N)} c_1^{-1} C_{T,\Gamma_N} |||\nabla(u-v)|||,$$

where C_{T,Γ_N} is a constant from the trace inequality such that

$$\|w\|_{L^2(\Gamma_N)} \leqslant C_{T,\Gamma_N}\|\nabla w\|_{L^2(\Omega)} \quad \text{for all } w \in V_0.$$

The factor ν can be chosen arbitrarily in the interval $(0,1)$. With $\nu = 0$ for $\kappa = 0$, we arrive at the estimate

$$\begin{aligned} I_3 \leqslant{}& \Big\|\frac{\nu}{\sqrt{\kappa}}(F - y\cdot n)\Big\|_{L^2(\Gamma_N)}\|\sqrt{\kappa}(u-v)\|_{L^2(\Gamma_N)} \\ &+ (1-\nu)\|(F - y\cdot n)\|_{L^2(\Gamma_N)}c_1^{-1}C_{T,\Gamma_N}|||\nabla(u-v)|||. \end{aligned} \tag{3.7}$$

We define

$$C_1 := c_1^{-1}C_{F,\Omega} \quad \text{and} \quad C_2 := c_1^{-1}C_{T,\Gamma_N}.$$

With (3.5)–(3.7) we obtain

$$\begin{aligned} |[u-v]|^2 \leqslant{}& \Big(\Big\|\frac{\mu}{\lambda}r_\Omega(v,y)\Big\|^2_{L^2(\Omega)} + |||y - A\nabla v|||^2_* + \Big\|\frac{\nu}{\sqrt{\kappa}}(F - y\cdot n)\Big\|^2_{L^2(\Gamma_N)}\Big)^{1/2} \\ &\times \big(\|\lambda(u-v)\|^2_{L^2(\Omega)} + |||\nabla(u-v)|||^2 + \|\sqrt{\kappa}(u-v)\|^2_{L^2(\Gamma_N)}\big)^{1/2} \\ &+ \big(C_1(1-\mu)\|r_\Omega(v,y)\|_{L^2(\Omega)} + C_2(1-\nu)\|(F - y\cdot n)\|_{L^2(\Gamma_N)}\big)|||\nabla(u-v)|||, \end{aligned}$$

which implies

$$\begin{aligned} |[u-v]| \leqslant{}& \Big(\Big\|\frac{\mu}{\lambda}r_\Omega(v,y)\Big\|^2_{L^2(\Omega)} + |||y - A\nabla v|||^2_* + \Big\|\frac{\nu}{\sqrt{\kappa}}(F - y\cdot n)\Big\|^2_{L^2(\Gamma_N)}\Big)^{1/2} \\ &+ C_1(1-\mu)\|r_\Omega(v,y)\|_{L^2(\Omega)} + C_2(1-\nu)\|(F - y\cdot n)\|_{L^2(\Gamma_N)}. \end{aligned} \tag{3.8}$$

The right-hand side of the general error majorant (3.8) contains three free parameters μ, ν, and y. It can be optimized with respect to them based on some numerical approximation u_h of the model problem (2.6).

In the following subsection, we demonstrate particular representations of this estimate which can be advantageous for different parameter settings of the reaction-convection-diffusion problem.

3.2. Particular Cases of the Error Majorant

One obtains particular forms of (3.8) by specific choices for the parameters μ and ν.

(a) For $\lambda^2 < 1$ and $\kappa < 1$, one can choose $\mu = \lambda$ and $\nu = \sqrt{\kappa}$. It follows

$$\begin{aligned} |[u-v]| \leqslant{}& \big(\|r_\Omega(v,y)\|^2_{L^2(\Omega)} + |||y - A\nabla v|||^2_* + \|(F - y\cdot n)\|^2_{L^2(\Gamma_N)}\big)^{1/2} \\ &+ C_1\|(1-\lambda)r_\Omega(v,y)\|_{L^2(\Omega)} + C_2\|(1-\sqrt{\kappa})(F - y\cdot n)\|_{L^2(\Gamma_N)}. \end{aligned}$$

(b) If the parameters λ^2 and κ exhibit large oscillations, the choice $\mu = \nu = 0$ can be beneficial. In this case, we obtain

$$|[u-v]| \leqslant |||y - A\nabla v|||_* + C_1\|r_\Omega(v,y)\|_{L^2(\Omega)} + C_2\|(F - y\cdot n)\|_{L^2(\Gamma_N)}.$$

This estimate does not contain λ^2 and κ to some negative power and, hence, is stable even for small values of these parameters.

(c) If the parameters λ^2 and κ exhibit large oscillations, one can additionally set $\nu = \sqrt{\kappa}$ and $\mu = \lambda$ in those parts of Ω where λ^2 and κ are small, e.g., see [14].

(d) Setting $\mu = \nu = 1$, we obtain

$$|[u-v]| \leqslant \Big(\Big\| \frac{1}{\lambda} r_\Omega(v,y) \Big\|^2_{L^2(\Omega)} + |||y - A\nabla v|||^2_* + \Big\| \frac{1}{\sqrt{\kappa}} (F - y\cdot n) \Big\|^2_{L^2(\Gamma_N)} \Big)^{1/2},$$

which is advantageous for reaction-convection-diffusion problems with dominant convection term. This estimation does not contain the constants from the trace and Friedrichs' inequalities and thus can be employed to obtain guaranteed bounds in many applications. Furthermore, it contains the constant c_1 to some negative power.

3.3. An Advanced Form of the Error Majorant

In practical applications it is useful to have an error estimation which is stable with respect to small values of λ^2 and κ but at the same time is applicable to problems with dominant convection. Such an error estimate is the main result in this paper.

Theorem 3.1 (A guaranteed stable energy norm a posteriori error estimator)**.** *Let u be the exact solution of problem* (2.1) *and let $v \in V_0 + u_0$, $y \in H(\Omega, \mathrm{div})$ and $\alpha, \beta \in \mathbb{R}$ be arbitrary. Then*

$$|[u-v]|^2 \leqslant \mathcal{M}^2_\Omega(v,y,\alpha,\beta) := \eta_{\mathrm{NB}} + \eta_{\mathrm{DF}} + \eta_{\mathrm{RES}}, \tag{3.9}$$

where the first term of the right-hand side comes from the boundary value estimation and is defined by

$$\eta_{\mathrm{NB}} := (1+\alpha)(1+\beta) \int_{\Gamma_N} \frac{C_2^2 (F - y\cdot n)^2}{\alpha(1+\beta) + \kappa C_2^2}\, ds.$$

The second term is related to the diffusion flux estimator and is given by

$$\eta_{\mathrm{DF}} := (1+\alpha)(1+\beta) |||y - A\nabla v|||^2_*.$$

The third term is a measure of the residual of the differential equation computed for an approximate solution v and a "flux" y and is defined by

$$\eta_{\mathrm{RES}} := (1+\alpha)(1+\beta) \int_\Omega \frac{C_1^2 r^2_\Omega(v,y)}{\beta + \lambda^2 C_1^2}\, dx.$$

Proof. To prove the theorem, we minimize the right-hand side of (3.8) with respect to the parameters μ and ν. We square the sum of the first two terms of (3.8) and employ Young's inequality with some positive β and note that the minimum of

$$(1+\beta)\mu^2 \int_\Omega \frac{1}{\lambda^2} r^2_\Omega(v,y)\, dx + \Big(1 + \frac{1}{\beta}\Big) C_1^2 (1-\mu)^2 \int_\Omega r^2_\Omega(v,y)\, dx$$

with regard to μ is equal to

$$\int_\Omega \frac{(\beta+1) C_1^2 r^2_\Omega(v,y)}{\beta + \lambda^2 C_1^2}\, dx.$$

This leads to

$$\begin{aligned} |[u-v]| \leqslant \sqrt{(1+\beta)\Big(|||y - A\nabla v|||^2_* + \nu^2 \int_{\Gamma_N} \frac{1}{\kappa} (F - y\cdot n)^2\, ds + \int_\Omega \frac{C_1^2 r^2_\Omega(v,y)}{\beta + \lambda^2 C_1^2}\, dx \Big)} \\ + C_2 (1-\nu) \|(F - y\cdot n)\|_{L^2(\Gamma_N)}. \end{aligned} \tag{3.10}$$

In order to optimize (3.10) with respect to ν, we again apply Young's inequality with a positive parameter and consider the terms containing the function ν. A straightforward calculation of the minimum of

$$(1+\alpha)\nu^2 \int_{\Gamma_N} \frac{1+\beta}{\kappa}(F - y\cdot n)^2\,ds + \Big(1+\frac{1}{\alpha}\Big)C_2^2(1-\nu)^2 \int_{\Gamma_N}(F-y\cdot n)^2\,ds$$

concludes the proof. □

3.4. Computation of the Majorant

To estimate the energy norm $|[u-v]|$, we need to evaluate the terms in (3.9) to obtain some flux approximation y as well as parameters α and β. For the diffusion equation, methods for the determination of β and the flux approximation y based on some discrete solution v have already been discussed in the literature (e.g., see [13,19,20,22,25]). Below we briefly discuss the application of these methods to our case. We emphasize that any choice $(\alpha,\beta,y) \subset \mathbb{R}\times\mathbb{R}\times H(\Omega,\mathrm{div})$ in the error majorant (3.9) results in a guaranteed upper bound of the error. However, sharp estimates require a sensible choice of these quantities. Moreover, a strategy needs to be devised which balances the extra computational cost with the benefit of sharper estimates. A possible approach is presented in this section.

If the values of A, a, F, f, and C_Ω are known then $\mathcal{M}^2_\Omega(v,y,\alpha,\beta)$ is a quadratic functional with respect to y. Our goal is to find some discrete $y_h \in V_h^2 \cap H(\Omega,\mathrm{div})$ and $\alpha,\beta\in\mathbb{R}$ such that $\mathcal{M}^2_\Omega(v,y_h,\alpha,\beta)$ is close to the minimum over $y\in H(\Omega,\mathrm{div})$. Minimization with respect to α and β is an algebraic problem. We introduce some additional notation for the corresponding iterative algorithm.

For every vertex $z\in\mathcal{N}$ of the triangulation $\mathcal{T}_h$, denote by $\mathcal{P}_z := \{\tau\in\mathcal{T}_h : z\in\overline{\tau}\}$ the neighboring elements. Moreover, $y_h^{(0)}\in V_h^2$ is defined implicitly from the patchwise flux averaging by the nodal condition

$$y_h^{(0)}(z) := \frac{1}{|\omega_z|}\int_{\omega_z} A\nabla v\,dx.$$

For all vertices $z_j\in\mathcal{N}$, $1\leqslant j\leqslant N$, let $\mathcal{M}^2_{\Omega,\omega_{z_j}}(v,y_h,\alpha,\beta)$ be the contribution of the patch ω_{z_j} to the majorant $\mathcal{M}^2_\Omega(v,y_h,\alpha,\beta)$. Algorithm 1 carries out a global optimization procedure in order to determine appropriate parameters for the error estimator.

Algorithm 1: Global minimization of the error majorant.

input : iterations $\nu_{\max}>0$
output: error majorant $\mathcal{M}^2_\Omega$
$y_h^{(0)}(z) \leftarrow \frac{1}{|\omega_z|}\int_{\omega_z} A\nabla v\,dx$
$\alpha^{(0)}\leftarrow 1$
$\beta^{(0)}\leftarrow 1$
for $\nu=1,\dots,\nu_{\max}$ **do**
1 $\quad y_h^{(\nu)} \leftarrow \operatorname{argmin}_{w\in V_h^2}\mathcal{M}^2_\Omega(v,w,\alpha^{(\nu-1)},\beta^{(\nu-1)})$
2 $\quad \alpha^{(\nu)} \leftarrow \operatorname{argmin}_{\alpha\in\mathbb{R}_+}\mathcal{M}^2_\Omega(v,y_h^\nu,\alpha,\beta^{(\nu-1)})$
3 $\quad \beta^{(\nu)} \leftarrow \operatorname{argmin}_{\beta\in\mathbb{R}_+}\mathcal{M}^2_\Omega(v,y_h^\nu,\alpha^{(\nu)},\beta)$
end
Calculate $\mathcal{M}^2_\Omega(v,y_h^{(\nu_{\max})},\alpha^{(\nu_{\max})},\beta^{(\nu_{\max})})$

With $\mathcal{M}^2_\Omega(v,y,\alpha,\beta)$ from (3.9), a minimization with respect to α according to line 2 in Algorithm 1 yields the relation

$$\int_{\Gamma_N} \frac{C_2^2(F-y\cdot n)^2(\kappa C_2^2-1-\beta)}{(\alpha(\beta+1)+\kappa C_2^2)^2}\,ds = -\int_\Omega \frac{C_1^2 r_\Omega^2(v,y)}{\beta+\lambda^2 C_1^2}\,dx - |||y-A\nabla v|||_*^2.$$

Similarly, for β in line 3 of Algorithm 1, we obtain

$$\int_{\Gamma_N} \frac{C_2^4\kappa(F-y\cdot n)^2}{(\alpha(\beta+1)+\kappa C_2^2)^2}\,ds + \int_\Omega \frac{C_1^2 r_\Omega^2(v,y)(\lambda^2 C_1^2-1)}{(\beta+\lambda^2 C_1^2)^2}\,dx = -|||y-A\nabla v|||_*^2.$$

A minimization of $\mathcal{M}^2_\Omega(v,y,\alpha,\beta)$ with respect to y according to line 1 in Algorithm 1 reveals

$$\begin{aligned}\int_{\Gamma_N} \frac{C_2^2\langle y\cdot n,\eta\cdot n\rangle}{\alpha(1+\beta)+\kappa C_2^2} + \int_\Omega \langle A^{-1}y,\eta\rangle + \int_\Omega \frac{C_1^2\langle \operatorname{div} y,\operatorname{div}\eta\rangle}{\beta+\lambda^2 C_1^2}\\ = \int_{\Gamma_N} \frac{C_2^2\langle F,\eta\cdot n\rangle}{\alpha(1+\beta)+\kappa C_2^2} + \int_\Omega \langle\nabla u_h,\eta\rangle - \int_\Omega \frac{C_1^2\langle \widetilde{f},\operatorname{div}\eta\rangle}{\beta+\lambda^2 C_1^2}\end{aligned} \tag{3.11}$$

with test functions η and $\widetilde{f} := f - a\cdot\nabla v - \rho^2 v$. We note that the global minimization in line 1 of Algorithm 1 requires the assembly and solution of a linear system (3.11) of dimension $2N$. On the one hand, we expect that the computational costs are of the same order as the cost to compute the discrete solution v. On the other hand, one could save memory (at the expense of less sharp estimates) if line 1 in Algorithm 1 would be replaced by a few steps of a Gauss–Seidel type iteration from line 1 of Algorithm 2.

In the following, an algorithm based on the solution of local minimization problems is depicted.

Algorithm 2: Local minimization of the error majorant.

input : iterations $\nu_{\max}, \iota_{\max} > 0$
output: error majorant $\mathcal{M}^2_\Omega$
$y_h^{(0)}(z) \leftarrow \frac{1}{|\omega_z|}\int_{\omega_z} A\nabla v\,dx$
$\alpha^{(0)} \leftarrow 1$
$\beta^{(0)} \leftarrow 1$
for $\nu = 1,\dots,\nu_{\max}$ **do**
  $\gamma_N^{(0)} \leftarrow y_h^{(\nu-1)}$
1 **for** $i = 1,\dots,\iota_{\max}$ **do**
    $\gamma_0^{(i)} \leftarrow \gamma_N^{(i-1)}$
    for $j = 1,\dots,N$ **do**
      $v_j \leftarrow \operatorname{argmin}_{w\in S_j^2} \mathcal{M}^2_{\Omega,\omega_{z_j}}(v,\gamma_{j-1}^{(i)}+w,\alpha^{(\nu-1)},\beta^{(\nu-1)})$
      $\gamma_j^{(i)} \leftarrow \gamma_{j-1}^{(i)} + w_j$
    end
  end
  $y_h^{(\nu)} \leftarrow \gamma_N^{(\iota_{\max})}$
  $\alpha^{(\nu)} \leftarrow \operatorname{argmin}_{\alpha\in\mathbb{R}_+} \mathcal{M}^2_\Omega(v,y_h^\nu,\alpha,\beta^{(\nu-1)})$
  $\beta^{(\nu)} \leftarrow \operatorname{argmin}_{\beta\in\mathbb{R}_+} \mathcal{M}^2_\Omega(v,y_h^\nu,\alpha^{(\nu)},\beta)$
end
Calculate $\mathcal{M}^2_\Omega(v,y_h^{(\nu_{\max})},\alpha^{(\nu_{\max})},\beta^{(\nu_{\max})})$

4. Numerical Examples

In this section, we present numerical examples for different coefficients which illustrate the performance of the a posteriori error estimator derived in Section 3. The chosen test cases can also be found in [7, 10, 15] which allows a direct comparison of the results.

For the numerical examples, we consider the second order equation (2.1) on the unit square $\Omega = (0,1) \times (0,1)$ with different diffusion values A and specific convection a and adsorption ρ^2 data such that the analytic solution is known. We focus on the more difficult and interesting case of dominant convection since the purely elliptic case has been treated exhaustively in previous publications. The Dirichlet boundary conditions are defined by some admissible sufficiently smooth u_0. In order to avoid instabilities due to dominating convection, the streamline diffusion method described in Section 2.2 is employed throughout.

In all numerical examples of the next subsections, the bulk marking (also known as Dörfler or greedy marking) based on the functional error estimator $\mathcal{M}_\Omega$ is applied. For some bulk parameter $0 < \Theta < 1$, the algorithm finds the smallest set of triangles $\tau \subset \mathcal{T}$ such that

$$\Theta \sum_{T \in \mathcal{T}} \mathcal{M}_\Omega(T) \leqslant \sum_{T \in \tau} \mathcal{M}_\Omega(T).$$

Here, $\mathcal{M}_\Omega(T) := \mathcal{M}_\Omega|_T$ is the restriction of the estimator onto any triangle $T \in \mathcal{T}$. Different marking strategies are possible and can lead to differently adapted meshes, see [15] for a study of several algorithms. The mesh is refined at least for the elements in τ with possible additional refinements to re-establish conformity of the mesh.

For the numerical results in this section, we assume $\Theta = 0.4$ and use Algorithm 1. We set $\alpha = 0.0001$ and choose

$$\beta = \Big(\frac{1 - \lambda^2 C_1^2}{|||y - A\nabla v|||_*^2}\Big)^{1/2} C_1 \|r_\Omega(v,y)\|_{L^2(\Omega)} - \lambda^2 C_1^2$$

for the minimization in line 3 of Algorithm 1.

4.1. Example 1

We consider problem (2.1) for the diffusion $A = \zeta I$ with different values $\zeta \in \mathbb{R}$, $a = (2,3)^T$, $\rho^2 = 2$, identity matrix I and $\Gamma_D = \partial\Omega$. The right-hand side and boundary conditions are chosen such that the exact solution is given by

$$u(x,y) = 16x(1-x)y(1-y)\Big(\frac{1}{2} + \frac{1}{\pi}\operatorname{atan}\Big(\frac{2}{\sqrt{A}}\Big(\frac{1}{16} - \Big(x - \frac{1}{2}\Big)^2 - \Big(y - \frac{1}{2}\Big)^2\Big)\Big)\Big).$$

The solution is plotted in Figure 1 (left). It exhibits a circular inner layer where the gradient depends on the diffusion and behaves like $O(\zeta^{-1/2})$.

Figure 2 shows the performance of the functional error estimator for different diffusion values, $A \in \{10^{-2}I, 10^{-4}I\}$.

We observe that in both cases the functional error estimator quickly exhibits optimal convergence rates. The efficiency index is close to 1 for $A = 10^{-2}I$ with 10^5 degrees of freedom and gets close to 10 for $A = 10^{-4}I$. In the energy norm, this dependence on the Péclet number is to be expected, see [7]. The plot of the adaptively refined mesh in Figure 1 (right) illustrates that the inner layer is resolved accurately. In Figure 3, the spatial error distribution as given by the error estimator and the exact solution is plotted. It shows a close resemblance qualitatively.

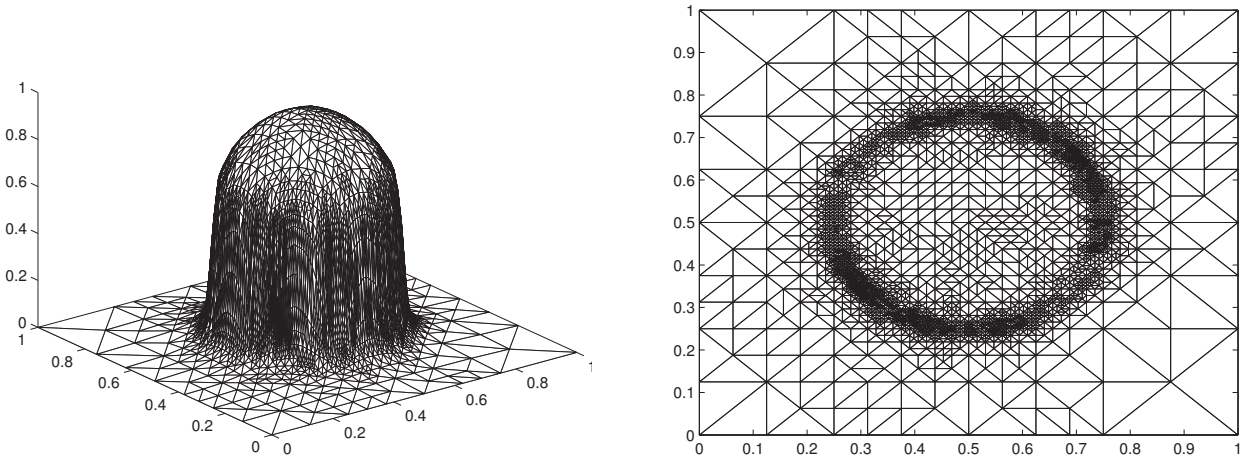

Figure 1. Example 1 solution (left) and adaptively refined mesh (right).

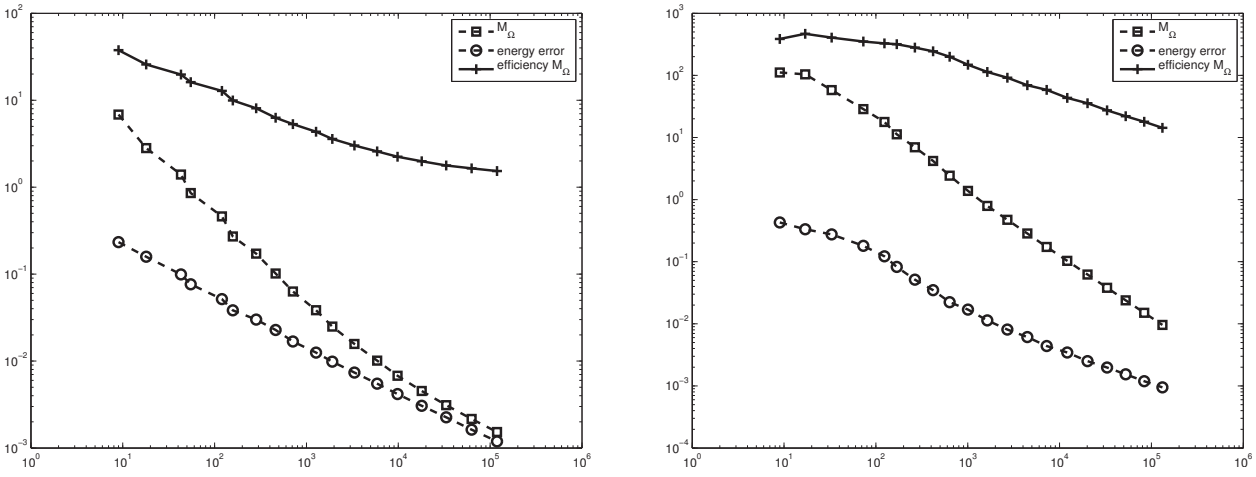

Figure 2. Energy error versus degrees of freedom for adaptive refinement: Example 1 with $A = 10^{-2}I$ (left) and $A = 10^{-4}I$ (right).

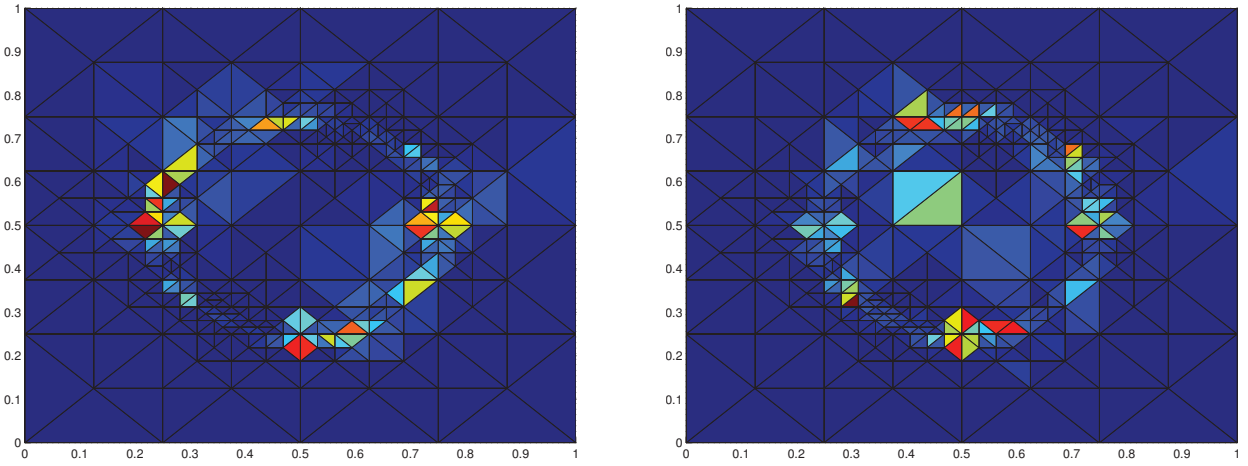

Figure 3. Error distribution in energy norm for Example 1 with $A = 10^{-4}I$ after seven iterations of the adaptive algorithm. Exact error (left) and error estimator (right); lighter color indicates larger error.

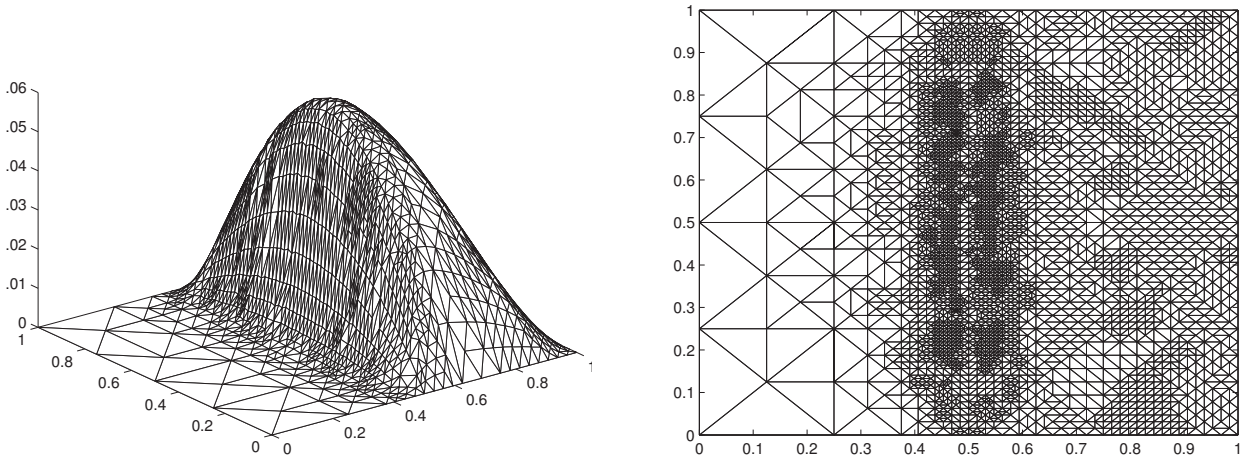

Figure 4. Example 2 solution (left) and refined mesh (right).

4.2. Example 2

We consider problem (2.1) with different values for ζ, $a = (1,0)^T$, $\rho^2 = 1$ and $\Gamma_D = \partial\Omega$. The right-hand side and boundary conditions are chosen such that the solution is given by

$$u(x,y) = \frac{1}{2}x(1-x)y(y-1)\big(1-\tanh(10-20x)\big).$$

The solution on an adaptively refined mesh is plotted in Figure 4 (right). The steep vertical gradient at the center of the domain is refined strongly.

Figure 5 shows the performance of the functional error estimator for different diffusion values, $A \in \{10^{-2}I, 10^{-4}I\}$.

The numerical results are comparable to the ones of Example 1. Again, the interior layer with steep gradients is resolved accurately. Moreover, the functional error estimator $\mathcal{M}_\Omega$ quickly reaches a good efficiency with respect to the Péclet number of the problem. Figure 6 depicts the spatial error distribution as given by the error estimator and the exact solution. Again, we see a close resemblance qualitatively.

4.3. Example 3

We consider problem (2.1) with $A = 10^{-2}I$, $a = (2,3)^T$, $\rho^2 = 1$ and $\Gamma_D = \partial\Omega$. The right-hand side and boundary conditions are chosen such that the solution is given by

$$u(x,y) = xy^2 - y^2\exp\Big(\frac{2(x-1)}{A}\Big) - x\exp\Big(\frac{3(y-1)}{A}\Big) + \exp\Big(\frac{2(x-1)+3(y-1)}{A}\Big).$$

The discrete solution on an adaptively refined mesh is plotted in Figure 7 (left). It exhibits boundary layers at the top and right-hand side of the domain. These layers are accurately resolved by the adaptive algorithm based on the functional error estimator $\mathcal{M}_\Omega$.

The convergence plots in Figure 7 (right) illustrate the stability of the functional error estimator. The error estimator $\mathcal{M}_\Omega$ exhibits optimal convergence rates almost immediately. Its efficiency is close to 1 even for relatively few degrees of freedom. Note that the boundary layers first have to be resolved sufficiently for the energy error to decrease significantly.

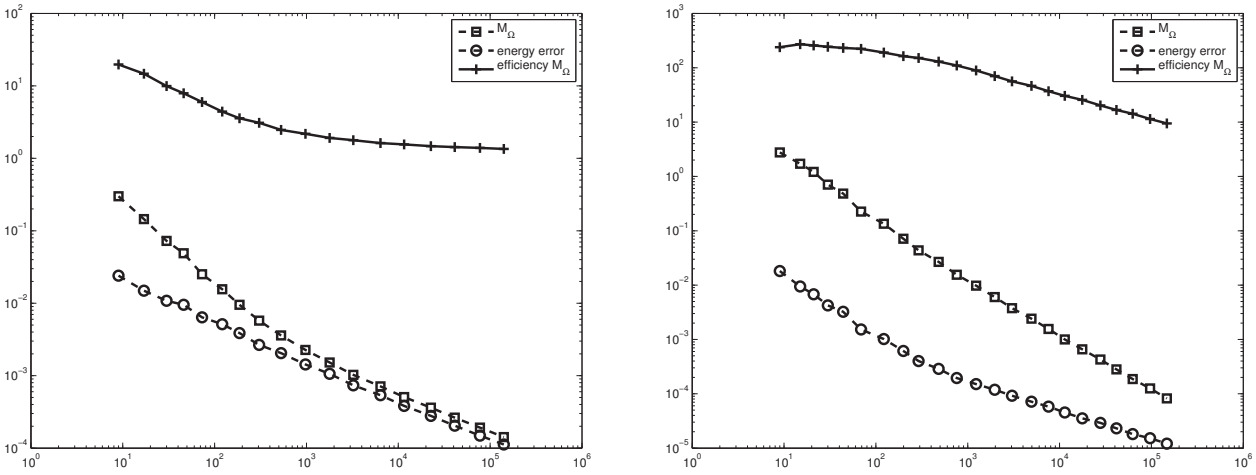

Figure 5. Energy error versus degrees of freedom for adaptive refinement: Example 2 with $A = 10^{-2}I$ (left) and $A = 10^{-4}I$ (right).

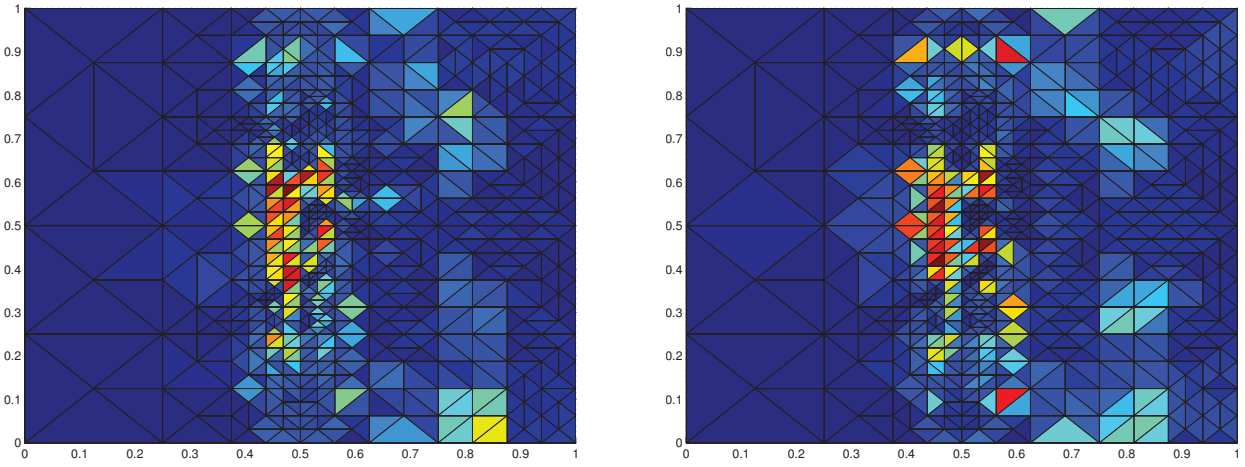

Figure 6. Error distribution in energy norm for Example 2 with $A = 10^{-4}I$ after ten iterations of the adaptive algorithm. Exact error (left) and error estimator (right); lighter color indicates larger error.

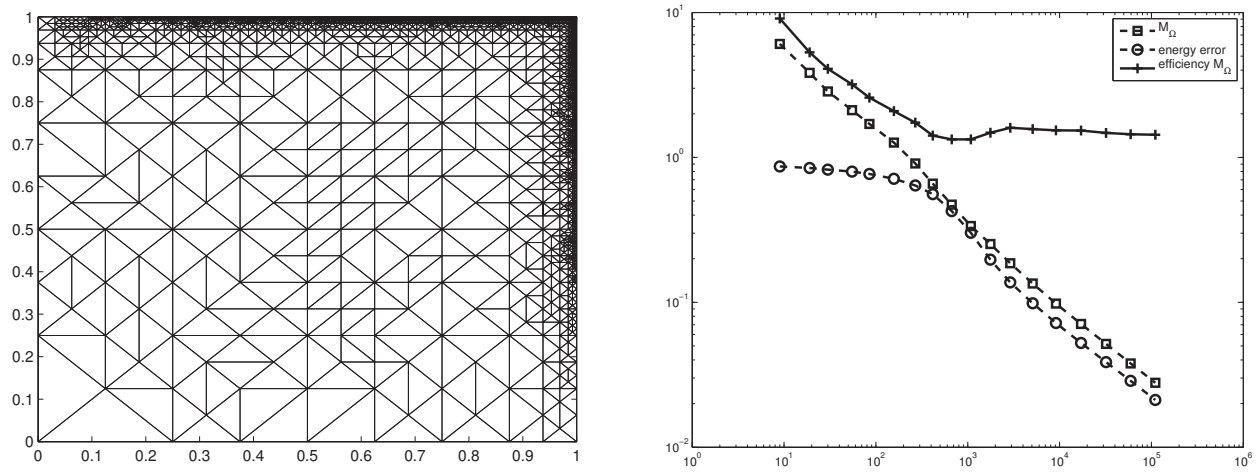

Figure 7. Example 3 adaptively refined mesh (left) and convergence for $A = 10^{-2}I$ with energy error versus degrees of freedom (right).

Acknowledgments

The authors would like to thank Prof. Sergey Repin and Dr. Christian Merdon for fruitful discussions and support with the implementation.

References

[1] R. A. Adams, *Sobolev Spaces*, Pure Appl. Math., 65, Academic Press, New York, 1975.

[2] M. Ainsworth and J. T. Oden, *A Posteriori Error Estimation in Finite Element Analysis*, Pure Appl. Math., Wiley-Interscience, New York, 2000.

[3] I. Babuška and T. Strouboulis, *The Finite Element Method and its Reliability*, Clarendon Press, Oxford, 2001.

[4] D. Braess, *Finite Elements*, 3rd edn., Cambridge University Press, Cambridge, 2007.

[5] S. C. Brenner and L. R. Scott, *The Mathematical Theory of Finite Element Methods*, 3rd edn., Texts Appl. Math., 15, Springer, New York, 2008.

[6] K. Eriksson and C. Johnson, *Adaptive streamline diffusion finite element methods for stationary convection-diffusion problems*, Math. Comp., **60** (1993), no. 201, pp. 167–188.

[7] A. Ern, A. F. Stephansen, and M. Vohralík, *Guaranteed and robust discontinuous Galerkin a posteriori error estimates for convection-diffusion-reaction problems*, J. Comput. Appl. Math., **234** (2010), no. 1, pp. 114–130.

[8] T. J. R. Hughes and A. Brooks, *A multidimensional upwind scheme with no crosswind diffusion*, in: Finite Element Methods for Convection Dominated Flows, AMD, 34, Amer. Soc. Mech. Engrs. (ASME), New York, 1979, pp. 19–35.

[9] T. J. R. Hughes, M. Mallet, and A. Mizukami, *A new finite element formulation for computational fluid dynamics. II. Beyond SUPG*, Comput. Methods Appl. Mech. Engrg., **54** (1986), no. 3, pp. 341–355.

[10] V. John, *A numerical study of a posteriori error estimators for convection-diffusion equations*, Comput. Methods Appl. Mech. Engrg., **190** (2000), no. 5–7, pp. 757–781.

[11] C. Johnson, *Adaptive finite element methods for diffusion and convection problems*, Comput. Methods Appl. Mech. Engrg., **82** (1990), no. 1–3, pp. 301–322.

[12] C. Johnson, U. Nävert, and J. Pitkäranta, *Finite element methods for linear hyperbolic problems*, Comput. Methods Appl. Mech. Engrg., **45** (1984), no. 1–3, pp. 285–312.

[13] P. Neittaanmäki and S. Repin, *Reliable Methods for Computer Simulation*, Stud. Math. Appl., 33, Elsevier, Amsterdam, 2004.

[14] S. Nicaise and S. Repin, *Functional a posteriori error estimates for the reaction-convection-diffusion problem*, Zap. Nauchn. Sem. S.-Peterburg. Otdel. Mat. Inst. Steklov. (POMI), **348** (2007), pp. 127–146.

[15] A. Papastavrou and R. Verfürth, *A posteriori error estimators for stationary convection-diffusion problems: A computational comparison*, Comput. Methods Appl. Mech. Engrg., **189** (2000), no. 2, pp. 449–462.

[16] S. Repin, *A posteriori error estimation for nonlinear variational problems by duality theory*, Zapiski Nauch. Semin. (POMI), **243** (1997), pp. 201–214.

[17] S. Repin, *A posteriori error estimation for variational problems with uniformly convex functionals*, Math. Comp., **69** (2000), pp. 481–600.

[18] S. Repin, *The estimates of the error of some two-dimensional models in the elasticity theory*, J. Math. Sci., **106** (2001), pp. 3027–3041.

[19] S. Repin, *Functional approach to locally based a posteriori error estimates for elliptic and parabolic problems*, in: Numerical Mathematics and Advanced Applications, Springer, Berlin, 2006, pp. 135–150.

[20] S. Repin, *A posteriori error estimation methods for partial differential equations*, in: Lectures on Advanced Computational Methods in Mechanics, Radon Ser. Comput. Appl. Math., 1, De Gruyter, Berlin, 2007, pp. 161–226.

[21] S. Repin, *Advanced forms of functional a posteriori error estimates for elliptic problems*, Russian J. Numer. Anal. Math. Modelling, **23** (2008), no. 5, pp. 505–521.

[22] S. Repin, *A Posteriori Estimates for Partial Differential Equations*, Radon Ser. Comput. Appl. Math., 4, De Gruyter, Berlin, 2008.

[23] S. Repin and T. Samrowski, *Estimates of dimension reduction errors for stationary reaction-diffusion problems*, J. Math. Sci. (N.Y.), **173** (2011), no. 6, pp. 803–821.

[24] S. Repin, T. Samrowski, and S. Sauter, *Combined a posteriori modeling-discretization error estimate for elliptic problems with complicated interfaces*, ESAIM Math. Model. Numer. Anal., **46** (2012), no. 6, pp. 1389–1405.

[25] S. Repin and S. Sauter, *Functional a posteriori estimates for the reaction-diffusion problem*, C. R. Math. Acad. Sci. Paris, **343** (2006), no. 5, pp. 349–354.

[26] R. Verfürth, *A Review of A Posteriori Error Estimation and Adaptive Mesh-Refinement Techniques*, John Wiley & Sons, Chichester, 1996.